

A substantial amount of hidden magnetic energy in the quiet Sun

J. Trujillo Bueno^{1,2}, N. Shchukina³ & A. Asensio Ramos¹

¹Instituto de Astrofísica de Canarias, E-38205 La Laguna, Tenerife, Spain

²Consejo Superior de Investigaciones Científicas, E-28006 Madrid, Spain

³Main Astronomical Observatory, National Academy of Sciences, Zabolotnoho 27, 03680 Kyiv, Ukraine

Deciphering and understanding the small-scale magnetic activity of the quiet solar photosphere should help to solve many of the key problems of solar and stellar physics, such as the magnetic coupling to the outer atmosphere and the coronal heating^{1–3}. At present, we can see only ~1 per cent of the complex magnetism of the quiet Sun^{1,4–7}, which highlights the need to develop a reliable way to investigate the remaining 99 per cent. Here we report three-dimensional radiative transfer modelling of scattering polarization in atomic and molecular lines that indicates the presence of hidden, mixed-polarity fields on subresolution scales. Combining this modelling with recent observational data^{8–11}, we find a ubiquitous tangled magnetic field with an average strength of ~130 G, which is much stronger in the intergranular regions of solar surface convection than in the granular regions. So the average magnetic energy density in the quiet solar photosphere is at least two orders of magnitude greater than that derived from simplistic one-dimensional investigations^{12,13}, and sufficient to balance radiative energy losses from the solar chromosphere.

Most of our present empirical knowledge of solar surface magnetism stems from the analysis of the light polarization that the Zeeman effect induces in spectral lines^{1,4–7}. For example, the circular polarization signals of which synoptic magnetograms are made reveal the existence of an irregular network of spatially unresolved, intermittent flux patches of kilogauss field concentrations outlining the boundaries of the giant velocity cells of the supergranulation¹. Such routine magnetograms give the (wrong) impression that the cell interiors (referred to here as internetwork regions) are non-magnetic, and it is important to note that such regions cover most of the solar ‘surface’ at any given time during the solar magnetic activity cycle. However, high-spatial-resolution magnetograms show a multitude of mixed magnetic polarities within the internetwork regions, with most of the detected flux located in the intergranular lanes of the solar granulation pattern where the plasma is downflowing^{4–7}. The mean unsigned flux density turns out to be ~10 G when choosing the best compromise between polarimetric sensitivity and spatio-temporal resolution that is at present feasible. When such polarization signals are interpreted taking into account the fact that the magnetic field is not being spatially resolved (for example, by assuming that one or more magnetic components are coexisting with a ‘non-magnetic’ component within the spatio-temporal resolution element of the observation), it is then found that the filling factor of the magnetic component(s) is ~1%. The ‘problem’ with the Zeeman effect is that the amplitudes of the measured polarization signals are smaller the greater the degree of cancellation of mixed magnetic polarities within the spatio-temporal resolution element of the observation. Therefore, lack of detection does not necessarily imply absence of magnetic fields.

Fortunately, scattering processes in spectral lines produce linear polarization signals, whose amplitudes are efficiently modified in the presence of tangled magnetic fields of strength $B_H \approx 1.137 \times 10^{-7} / (t_{\text{life}} g_L)$ (with B_H expressed in gauss, and where t_{life} and g_L are respectively the lifetime in seconds and Landé factor of the upper level of the transition). This so-called Hanle effect^{14,15} has the required diagnostic potential for investigating spatially unresolved, ‘hidden’ mixed-polarity magnetic fields

in the solar atmosphere¹⁶. The problem is how to apply it to obtain reliable information, given that Hanle-effect diagnostics of such ‘turbulent’ fields rely on a comparison between the observed scattering polarization and that corresponding to the zero-field reference case. It has been pointed out correctly^{12,13} that a suitable spectral line for Hanle-effect diagnostics of ‘turbulent’ photospheric fields is that of Sr I at 4,607 Å. However, the simplified approach of assuming that the highly inhomogeneous and dynamic solar photosphere can be well represented by a one-dimensional (1D) and static model is very unreliable, because of the need to use the free parameters of ‘classical’ stellar spectroscopy (that is, micro- and macroturbulence for line broadening), which have a serious impact on the calculated polarization amplitudes¹⁷. We have shown¹⁷ that the particular 1D approach that has been applied^{12,13} yields artificially low values for the strength of the ‘turbulent’ field—that is, between 20 and 10 G as shown by the dashed lines of Fig. 3 in ref. 17.

In order to improve the reliability of diagnostic tools based on the Hanle effect, we have developed a novel approach based on multi-level scattering polarization calculations in three-dimensional (3D) models of the solar photosphere, which we have obtained from realistic hydrodynamical simulations of solar surface convection¹⁸. This has allowed us to obtain the linear polarization amplitudes that scattering processes in the inhomogeneous solar photosphere would produce in the Sr I 4,607 Å line if there were no magnetic

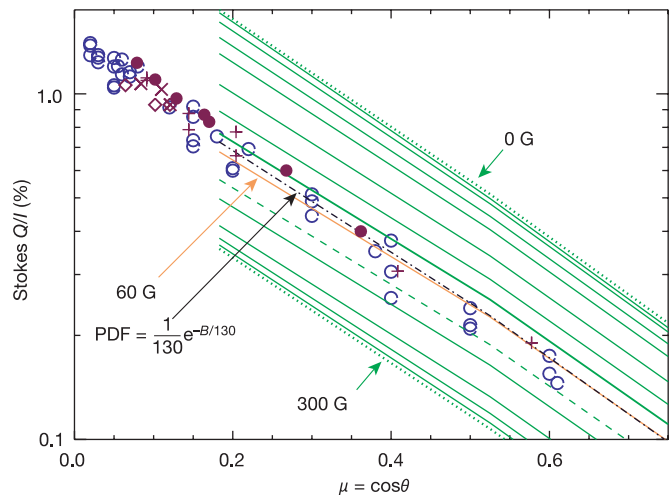


Figure 1 Spectropolarimetric observations versus 3D modelling of the Hanle effect. This figure shows the centre-to-limb variation of the fractional linear polarization at the core of the Sr I 4,607 Å line after subtraction of the continuum polarization level. (The Stokes I and Q parameters are defined in ref. 1; $\mu = \cos\theta$, with θ the angle between the solar radius vector through the observed point and the line of sight.) Open circles, various observations⁸ taken during a minimum period of the solar cycle (in particular, during September–October 1995). The remaining symbols correspond to observations taken during the most recent maximum period of the solar cycle. Diamonds, observations⁹ obtained during May 2000; crosses and ‘plus’ symbols, observations taken during August 2000 (see ref. 10) and December 2002 (V. Bommier; personal communication), respectively; filled circles, observations obtained during September 2003 at the Istituto Ricerche Solari Locarno (Switzerland) in collaboration with M. Bianda. Coloured lines, the results of our 3D scattering polarization calculations in the presence of a volume-filling and single-valued microturbulent field with an isotropic distribution of directions below the mean free path of the line photons (from top to bottom: 0, 5, 10, 15, 20, 30, 40, 50, 60, 80, 100, 150, 200, 250 and 300 G). We have solved the relevant equations²⁸ via the application of efficient radiative transfer methods²⁹, and using realistic collisional depolarizing rate values¹², which turn out to be the largest rates among those found in the literature. Note that there is no evidence of a serious modulation of the strength of the ‘turbulent’ field with the last solar activity cycle, and that the best average fit to the observations is obtained for 60 G. The black dashed-dotted line indicates the resulting Q/I line-core amplitudes for the case of a single exponential PDF ($e^{-B/B_0} / B_0$) with $B_0 = 130$ G, which implies $\langle B \rangle = 130$ G.

field. We point out that our synthetic intensity profiles (which take fully into account the Doppler shifts of the convective flow velocities in the 3D model) are automatically in excellent agreement with the observations when the meteoritic strontium abundance is chosen. However, we find that the calculated fractional linear polarization is substantially larger than the observed one, thus indicating the need to invoke magnetic depolarization.

As seen in Fig. 1, our radiative transfer simulations of the Hanle effect in the Sr I line show that a volume-filling, microturbulent magnetic field of about 60 G leads to a notable agreement with the observed Q/I (where Q and I are Stokes parameters). In Fig. 1 there

is a clear indication that the strength of the ‘turbulent’ field required to explain the Q/I observations decreases with height in the atmosphere, from the 70 G needed to explain the observations at $\mu = 0.6$ to the 50 G required to fit the observations at $\mu = 0.1$ (μ is defined in Fig. 1 legend). This corresponds approximately to a height range between 200 and 400 km above the solar visible ‘surface’.

If the hidden magnetic field of the quiet solar photosphere really had a strength of 60 G at all points in the solar photosphere, then the mean magnetic energy density ($E_m = \langle B^2 \rangle / 8\pi$) would be $E_m \approx 140 \text{ erg cm}^{-3}$, which is an order of magnitude smaller than that corresponding to the kilogauss fields of the network patches.

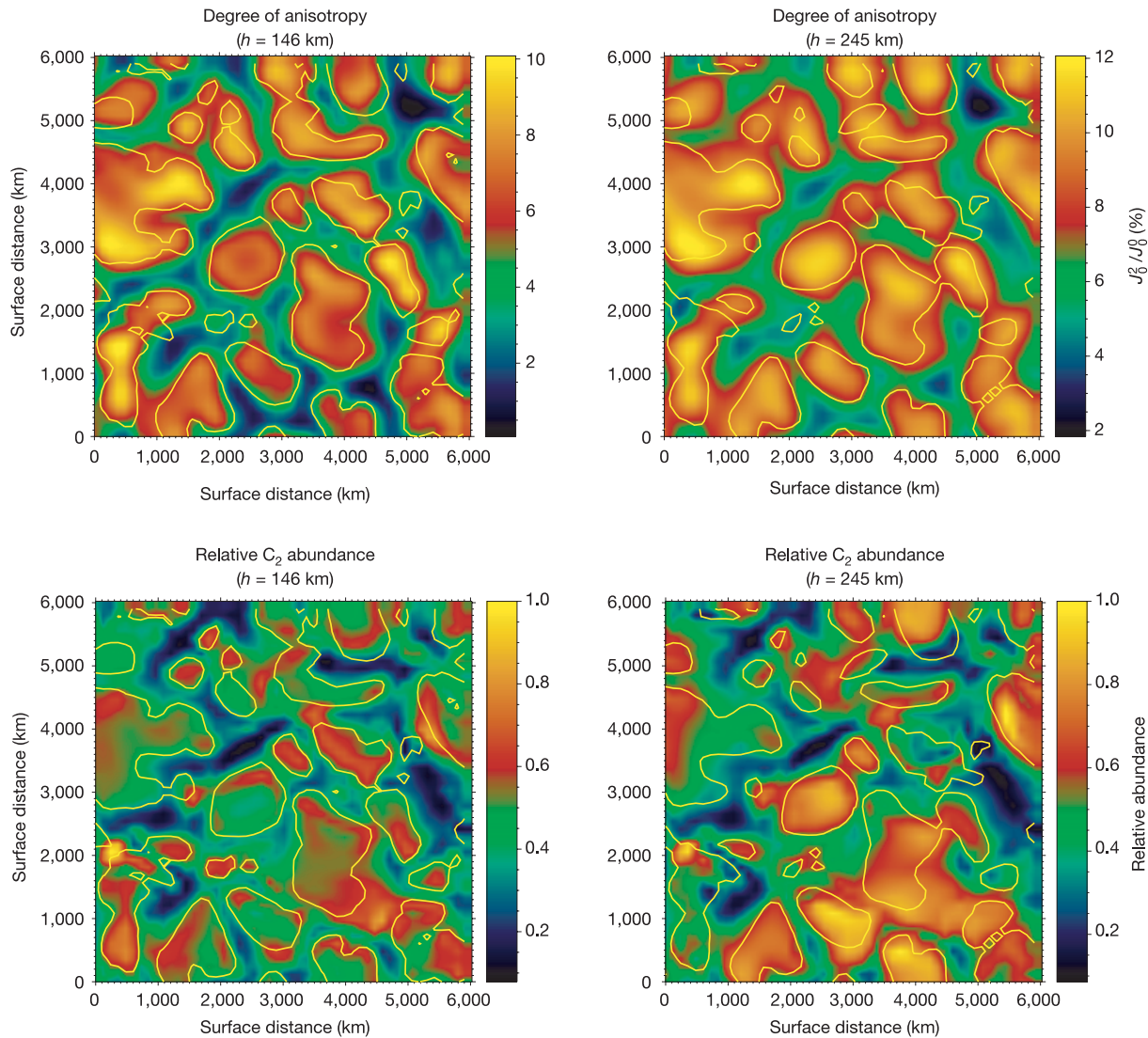


Figure 2 Evidence for a ‘turbulent’ field organized at the spatial scales of the solar granulation pattern. This figure demonstrates that the scattering polarization observed in molecular lines¹¹ comes mainly from the upflowing regions of the ‘quiet’ solar photosphere. The solid line contours delineate such upflowing regions at two heights (h) in the 3D photospheric model, which indicate the approximate atmospheric region where the observed C_2 line radiation originates. The two top panels show the horizontal fluctuation of the ‘degree of anisotropy’ ($\mathcal{A} = J_0^2/J_0^0$; refs 15, 28) of the solar continuum radiation at 5,000 Å. (Note that there is a very strong correlation between the upflowing regions and \mathcal{A} .) The two bottom panels visualize the corresponding horizontal fluctuation in the number density (\mathcal{N}) of C_2 molecules. (Note that there is a significant correlation between the upflowing regions and \mathcal{N} .) As in the solar atmosphere the scattering polarization in weak molecular lines is proportional to both \mathcal{A} and \mathcal{N}/η_c (where η_c is the

background continuum opacity, which is anticorrelated with \mathcal{N} in such a range of heights) we conclude that only the upflowing regions make a significant contribution to the observed molecular scattering polarization. Therefore, we can obtain information on the distribution of magnetic fields in such (granular) upflowing regions of the solar photosphere via theoretical modelling of the observed scattering polarization in suitably chosen pairs of C_2 lines³⁰. We have calculated the magnetic sensitivity of the observed C_2 lines by taking into account all the relevant optical pumping mechanisms in a very realistic multilevel model for C_2 . Thanks to this Hanle-effect investigation, we have been able to conclude that in the granular regions the ‘turbulent’ field is much weaker than what is needed to explain the observed depolarization in the Sr I 4,607 Å line. For this reason, the intergranular regions must be pervaded by relatively strong tangled fields capable of producing most of the observed depolarization in the strontium line.

However, both magnetohydrodynamical simulations^{19,20} and observations of the Zeeman effect^{4,21,7} indicate that the photospheric plasma of the quiet Sun has a continuous distribution of field strengths, in such a way that the weaker the field the larger the probability of finding a magnetic strength between B and $B + dB$ when no distinction is made between granular and intergranular regions. As shown by the black dashed-dotted line of Fig. 1, if we assume that the probability distribution function (PDF) has an exponential shape ($e^{-B/B_0}/B_0$), we then find that $B_0 \approx 130$ G yields a fairly good fit to the observed fractional linear polarization. In this much more realistic case $E_m \approx 1,300$ erg cm⁻³ (that is, $\sqrt{\langle B^2 \rangle} \approx 180$ G), which is about 20% of the averaged kinetic energy density produced by convective motions at a height of 200 km in the 3D photospheric model. This result and the fact that the observed Q/I does not seem to be modulated by the solar cycle (see Fig. 1) suggests that a small-scale dynamo associated with turbulent motions within a given convective domain of ionized gas^{19,20} plays a significant role for the quiet Sun magnetism. The total magnetic energy stored in the internetwork regions is now slightly larger than that corresponding to the kilogauss fields of the network patches. It is also of interest to point out that our empirical PDF with $\langle B \rangle \approx 130$ G produces a negligible Zeeman broadening of the emergent spectral line profiles, which is fully compatible with the reported empirical constraints¹. However, in contrast to what might be expected from the conclusions of a recent paper²², the stretched exponential PDF that characterizes the surface distribution of magnetic fields ‘predicted’ by the most recent numerical experiments of turbulent dynamos¹⁹, which correspond to a magnetic Reynolds number of about 1,000, implies a Hanle-effect reduction of the scattering polarization amplitude of the Sr I 4,607 Å line that is significantly smaller than what is needed to explain the observations.

We do not have a sufficient number of observational constraints to be able to determine the exact shape or the detailed spatial variation of the solar PDF. However, we can conclude that the ‘turbulent’ field is organized at the spatial scales of the solar granulation pattern, with relatively weak fields above the granules and with much stronger fields above the intergranular lanes (Fig. 2). As shown in Fig. 2 legend, most of the volume of the upflowing granules where the observed C₂ line polarization originates is occupied by magnetic fields much weaker than what is needed to explain the observed depolarization in the Sr I 4,607 Å line. Therefore, most (but not all) of the observed strontium line depolarization must be produced by relatively strong and tangled fields in the intergranular regions.

The contribution of the intergranular plasma to the observed scattering polarization in the strontium line is very likely to be close to the regime of Hanle saturation, which for this spectral line occurs for magnetic strengths $B \gtrsim 300$ G (Fig. 1). This helps us to understand why, with low spatial and temporal resolution, it is not easy (but definitely not impossible) to detect spatial fluctuations in the observed Q/I (Fig. 1). We have carried out calculations with several plausible PDFs, assuming in all cases that the angular distribution of the field vectors is isotropic and microturbulent for every single field strength. For instance, we have assumed an exponential PDF ($\text{PDF}_G = e^{-B/B_g}/B_g$) for the upflowing regions with a free parameter B_g to be determined from the observations and a given maxwellian function ($\text{PDF}_I = 2.38 \times 10^{-8} B^2 \exp(-B/456)^2$) for the downflowing plasma obtained from a best fit to the strong field part of the intergranular histogram of the Zeeman splittings observed in near-infrared lines of neutral iron⁷. Note that this maxwellian PDF implies that the filling factor of kilogauss fields is $\sim 2\%$ —that is, it does not exclude the possibility⁶ of small-scale kilogauss fields in the internetwork regions. With this ‘educated’ choice of plausible PDFs, the best agreement between theory and observations is obtained for $B_g \approx 15$ G, which is consistent with the results of our investigation of the Hanle effect in C₂ lines. We find

that most of the magnetic energy turns out to be due to rather chaotic fields in the intergranular plasma with strengths between the equipartition field values and ~ 1 kG. The total magnetic energy stored in the internetwork regions is now substantially larger than that corresponding to the kilogauss fields of the supergranulation network.

Our conclusion that most of the volume of the granular regions is occupied by very weak fields seems to be compatible with the constraints imposed by our present understanding²³ of the ‘enigmatic’ scattering polarization observed in the Na I D₁ line, whose line-core radiation originates a few hundred kilometres higher in the solar atmosphere. As demonstrated in ref. 23, the linear polarization signature of the scattered light in the D₁ line is only completely suppressed in the presence of magnetic fields larger than 10 G, regardless of their inclination. Note that this result is significantly different to what had been concluded in an earlier paper²⁴. In any case, it is important to point out that the observed linear polarization in the sodium D₁ line still remains enigmatic because nobody has yet been able to model both the amplitude and shape of the observed Q/I profile²⁵.

Our empirical findings may have far-reaching implications in solar and stellar physics. The hot outer regions of the solar atmosphere (chromosphere and corona) radiate and expand, which takes energy. By far the largest energy losses stem from chromospheric radiation, with a total energy flux of $\sim 10^7$ erg cm⁻² s⁻¹. Considering our most conservative estimate for the magnetic energy density — that is, $E_m \approx 140$ erg cm⁻³ — we obtain an energy flux similar to the above-mentioned chromospheric energy losses when using either the typical value of ~ 1 km s⁻¹ for the convective velocities or the Alfvén speed ($v_A = B/(4\pi\rho)^{1/2}$, with ρ the gas density). In reality, as pointed out above, the true magnetic energy density that at any given time during the solar cycle is stored in the quiet solar photosphere is very much larger than 140 erg cm⁻³. Only a relatively small fraction would thus suffice to balance the energy losses of the solar outer atmosphere.

Equally interesting is our result that $\langle B \rangle \approx 130$ G, which indicates that the unsigned magnetic flux density in the quiet solar photosphere is substantially large. In fact, it has been suggested recently that the dynamic geometry of the magnetic connection between the photosphere and the corona may sensitively depend on the amount of magnetic flux that exists in the internetwork regions³. The hidden flux that we have diagnosed turns out to be organized at the spatial scales of the solar granulation pattern, with much stronger fields in the intergranular regions. Therefore, if the magnetic field of the ‘quiet’ solar chromosphere is found to be more complex than simply canopy-like, because of the influence of the intergranular magnetic fields which are continuously moving around on temporal scales of minutes, then the possibilities for magnetic reconnection²⁷ and energy dissipation in the solar outer atmosphere would be much enhanced. The ‘hidden’ magnetic fields that we have reported here could thus provide the clue to understanding how the 10⁶ K solar corona is heated. □

Received 13 January; accepted 17 May 2004; doi:10.1038/nature02669.

1. Stenflo, J. O. *Solar Magnetic Fields: Polarized Radiation Diagnostics* (Kluwer, Dordrecht, 1994).
2. Schrijver, C. J. *et al.* Large-scale coronal heating by the small-scale magnetic field of the Sun. *Nature* **394**, 152–154 (1998).
3. Schrijver, C. J. & Title, A. The magnetic connection between the solar photosphere and the corona. *Astrophys. J.* **597**, L165–L168 (2003).
4. Lin, H. & Rimmele, T. The granular magnetic fields of the quiet Sun. *Astrophys. J.* **514**, 448–455 (1999).
5. Sánchez Almeida, J. & Lites, B. Physical properties of the solar magnetic photosphere under the MISMA hypothesis. II. Network and internetwork fields at the disk center. *Astrophys. J.* **532**, 1215–1229 (2000).
6. Domínguez Cerdeña, I., Kneer, F. & Sánchez Almeida, J. Quiet-Sun magnetic fields at high spatial resolution. *Astrophys. J.* **582**, L55–L58 (2003).
7. Khomenko, E., Collados, M., Solanki, S. K., Lagg, A. & Trujillo Bueno, J. Quiet-Sun internetwork magnetic fields observed in the infrared. *Astron. Astrophys.* **408**, 1115–1135 (2003).
8. Stenflo, J. O., Bianda, M., Keller, C. & Solanki, S. K. Center-to-limb variation of the second solar spectrum. *Astron. Astrophys.* **322**, 985–994 (1997).

9. Trujillo Bueno, J., Collados, M., Paletou, F. & Molodij, G. in *Advanced Solar Polarimetry: Theory, Observations and Instrumentation* (ed. Sigwarth, M.) 141–149 (ASP Conf. Ser. Vol. 236, Astronomical Society of the Pacific, San Francisco, 2001).
10. Bomnier, V. & Molodij, G. Some THEMIS-MTR observations of the second solar spectrum (2000 campaign). *Astron. Astrophys.* **381**, 241–252 (2002).
11. Gandorfer, A. *The Second Solar Spectrum* Vol. 1, 4625 Å to 6995 Å (vdf, Zurich, 2000).
12. Faurobert-Scholl, M., Feautrier, N., Machefert, F., Petrovay, K. & Spielfiedel, A. Turbulent magnetic fields in the solar photosphere: diagnostics and interpretation. *Astron. Astrophys.* **298**, 289–302 (1995).
13. Faurobert, M., Arnaud, J., Vigneau, J. & Frisch, H. Investigation of weak solar magnetic fields. New observational results for the Sr I 460.7 nm linear polarization and radiative transfer modeling. *Astron. Astrophys.* **378**, 627–634 (2001).
14. Hanle, W. Über magnetische Beeinflussung der Polarisation der Resonanzfluoreszenz. *Z. Phys.* **30**, 93–105 (1924).
15. Trujillo Bueno, J. in *Advanced Solar Polarimetry: Theory, Observations and Instrumentation* (ed. Sigwarth, M.) 161–195 (ASP Conf. Ser. Vol. 236, Astronomical Society of the Pacific, San Francisco, 2001).
16. Stenflo, J. O. The Hanle effect and the diagnostics of turbulent magnetic fields in the solar atmosphere. *Sol. Phys.* **80**, 209–226 (1982).
17. Shchukina, N. & Trujillo Bueno, J. in *Solar Polarization 3* (eds Trujillo Bueno, J. & Sánchez Almeida, J.) 336–343 (ASP Conf. Ser. Vol. 307, Astronomical Society of the Pacific, San Francisco, 2003).
18. Asplund, M., Nordlund, Å., Trampedach, R., Allende Prieto, C. & Stein, R. F. Line formation in solar granulation. I. Fe line shapes, shifts and asymmetries. *Astron. Astrophys.* **359**, 729–742 (2000).
19. Cattaneo, F. On the origin of magnetic fields in the quiet photosphere. *Astrophys. J.* **515**, L39–L42 (1999).
20. Stein, R. F. & Nordlund, Å. in *Modelling of Stellar Atmospheres* (eds Piskunov, N. E., Weiss, W. W. & Gray, D. F.), 169–180 (ASP Conf. Ser. Vol. IAU 210, Astronomical Society of the Pacific, San Francisco, 2003).
21. Socas-Navarro, H. & Sánchez Almeida, J. Magnetic fields in the quiet Sun: observational discrepancies and unresolved structure. *Astrophys. J.* **593**, 581–586 (2003).
22. Sánchez Almeida, J., Emonet, T. & Cattaneo, F. Polarization of photospheric lines from turbulent dynamo simulations. *Astrophys. J.* **585**, 536–552 (2003).
23. Trujillo Bueno, J., Casini, R., Landolfi, M. & Landi Degl'Innocenti, E. The physical origin of the scattering polarization of the Na I D lines in the presence of weak magnetic fields. *Astrophys. J.* **566**, L53–L57 (2002).
24. Landi Degl'Innocenti, E. Evidence against turbulent and canopy-like magnetic fields in the solar chromosphere. *Nature* **392**, 256–258 (1998).
25. Stenflo, J. O. in *Solar Polarization 3* (eds Trujillo Bueno, J. & Sánchez Almeida, J.) 385–398 (ASP Conf. Ser. Vol. 307, Astronomical Society of the Pacific, San Francisco, 2003).
26. Anderson, L. S. & Athay, R. G. Model solar chromosphere with prescribed heating. *Astrophys. J.* **346**, 1010–1018 (1989).
27. Priest, E. & Forbes, T. *Magnetic Reconnection: MHD Theory and Applications* (Cambridge Univ. Press, New York, 2000).
28. Landi Degl'Innocenti, E. Polarization in spectral lines: I. A unifying theoretical approach. *Sol. Phys.* **85**, 3–31 (1983).
29. Trujillo Bueno, J. in *Stellar Atmosphere Modeling* (eds Hubeny, I., Mihalas, D. & Werner, K.) 551–582 (ASP Conf. Ser. Vol. 288, Astronomical Society of the Pacific, San Francisco, 2003).
30. Trujillo Bueno, J. in *Solar Polarization 3* (eds Trujillo Bueno, J. & Sánchez Almeida, J.) 407–424 (ASP Conf. Ser. Vol. 307, Astronomical Society of the Pacific, San Francisco, 2003).

Acknowledgements We thank F. Kneer, E. Landi Degl'Innocenti and F. Moreno-Insertis for scientific discussions. We are also grateful to P. Fabiani Bendicho for help with the numerical solution of the 3D radiative transfer equation. This research was supported by the Spanish Plan Nacional de Astronomía y Astrofísica and by the European Commission via the INTAS programme and the Solar Magnetism Network.

Competing interests statement The authors declare that they have no competing financial interests.

Correspondence and requests for materials should be addressed to J.T.B. (jtb@iac.es).

Single spin detection by magnetic resonance force microscopy

D. Rugar, R. Budakian, H. J. Mamin & B. W. Chui

IBM Research Division, Almaden Research Center, 650 Harry Rd, San Jose, California 95120, USA

Magnetic resonance imaging (MRI) is well known as a powerful technique for visualizing subsurface structures with three-dimensional spatial resolution. Pushing the resolution below 1 μm remains a major challenge, however, owing to the sensitivity limitations of conventional inductive detection techniques. Currently, the smallest volume elements in an image must contain at least 10¹² nuclear spins for MRI-based microscopy¹, or 10⁷

electron spins for electron spin resonance microscopy². Magnetic resonance force microscopy (MRFM) was proposed as a means to improve detection sensitivity to the single-spin level, and thus enable three-dimensional imaging of macromolecules (for example, proteins) with atomic resolution^{3,4}. MRFM has also been proposed as a qubit readout device for spin-based quantum computers^{5,6}. Here we report the detection of an individual electron spin by MRFM. A spatial resolution of 25 nm in one dimension was obtained for an unpaired spin in silicon dioxide. The measured signal is consistent with a model in which the spin is aligned parallel or anti-parallel to the effective field, with a rotating-frame relaxation time of 760 ms. The long relaxation time suggests that the state of an individual spin can be monitored for extended periods of time, even while subjected to a complex set of manipulations that are part of the MRFM measurement protocol.

MRFM is based on the detection of the magnetic force between a ferromagnetic tip and spins in a sample. The fundamental challenge in achieving single-spin sensitivity is that the force from a single spin is exceedingly small. Even with tip field gradients in the gauss per nanometre range, the force from an electron spin is only a few attonewtons. This force is roughly a million times smaller than is typically detected by atomic force microscopy (AFM). Recently, major strides towards single-spin detection have been made with the development of ultrasensitive cantilever-based force sensors^{7,8}, better understanding of relevant spin relaxation processes^{9–12} and the successful detection of statistical polarization in small spin ensembles¹³.

The basic elements of our MRFM apparatus are shown in Fig. 1 and have been described in detail in ref. 13. Briefly, a custom-fabricated mass-loaded silicon cantilever^{8,13} with an attached 150-nm-wide SmCo magnetic tip is used to sense the force from the electron spin. The sample consists of vitreous silica (Suprasil W2) that was irradiated with a 2-Gy dose of Co⁶⁰ gamma rays. The gamma irradiation produces a low concentration of silicon dangling bonds containing unpaired electron spins known as E' centres¹⁴.

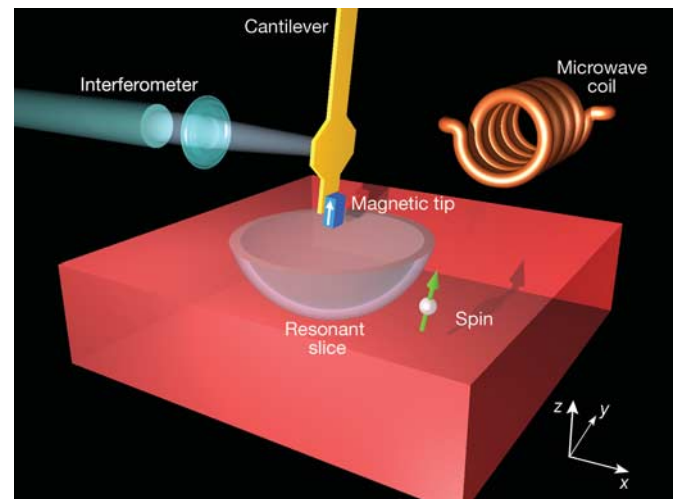


Figure 1 Configuration of the single-spin MRFM experiment. The magnetic tip at the end of an ultrasensitive silicon cantilever is positioned approximately 125 nm above a polished SiO₂ sample containing a low density of unpaired electron spins. The resonant slice represents those points in the sample where the field from the magnetic tip (plus an external field) matches the condition for magnetic resonance. As the cantilever vibrates, the resonant slice swings back and forth through the sample causing cyclic adiabatic inversion of the spin. The cyclic spin inversion causes a slight shift of the cantilever frequency owing to the magnetic force exerted by the spin on the tip. Spins as deep as 100 nm below the sample surface can be probed.